Supporting Information

Identification of Charge Separated States in Thymine Single Strands

Bert M. Pilles, Dominik B. Bucher, Lizhe Liu, Peter Gilch, Wolfgang Zinth, Wolfgang J. Schreier

Table of contents

1. Material and Methods

The oligomer $(dT)_{18}$ was purchased from Eurogentec, TpA from Metabion, TMP and thymine from Sigma Aldrich. The samples were obtained as lyophilized powders and were used without further purification. All samples were dissolved in phosphate buffered D_2O solutions (50 mM, pD ~ 7) to yield concentrations of about 10 mM (per Base).

The time resolved infrared (TRIR) instrument is described in refs. [1-3]. In brief, the instrument is based on a Ti:saphire CPA system (Spitfire Pro XP) yielding 100 fs pulses at 800 nm with at a repetition rate of 1kHz. The third harmonic (266 nm) of the fundamental was used for excitation of the samples. Thereby, the excitation energy was set to 2 μJ at a diameter of ca. 150 μm (fwhm). The probe pulses were generated using a combination of a collinear and a non-collinear optical parametric amplifier with subsequent difference frequency mixing in a $AgGaS_2$ crystal. The resulting mid-IR pulses (probe and reference) were spectrally dispersed (Bruker Chromex 250is) and detected by two 64-Channel MCT arrays (Infrared Associates Inc.) connected to a multichannel data acquisition system (IR 0144, Infrared Systems Development Corp.). All measurements were performed under magic angle conditions.

For ns-experiments, the samples were excited at 266 nm with an electronically synchronised Nd:YVO laser (fourth harmonic of a AOT-YVO-25QSP/MOPA, Advanced Optical Technology Ldt.) as detailed in refs.[2, 4].
In all time resolved experiments the samples were held in flow cells (pathlength ~100 μm, BaF_2-windows), and the sample volume was exchanged between consecutive excitation pulses.

2. Raw Data and Corrections

Figure S1 shows the raw data of the measurement on $(dT)_{18}$. In the upper panel a contour plot of the recorded absorption difference data gives an overview of the spectral and temporal range monitored. In the lower panel transient spectra at delay times of 20 ps (black line) and 500 ps (red line) are depicted. The data show that absorption changes with considerable amplitudes occur on the 100 ps time scale. The signals at the late times are composed of absorption changes due to heating of the solvent, triplet formation, CPD formation and possibly other long-lived states (e.g. $n\pi^*$).

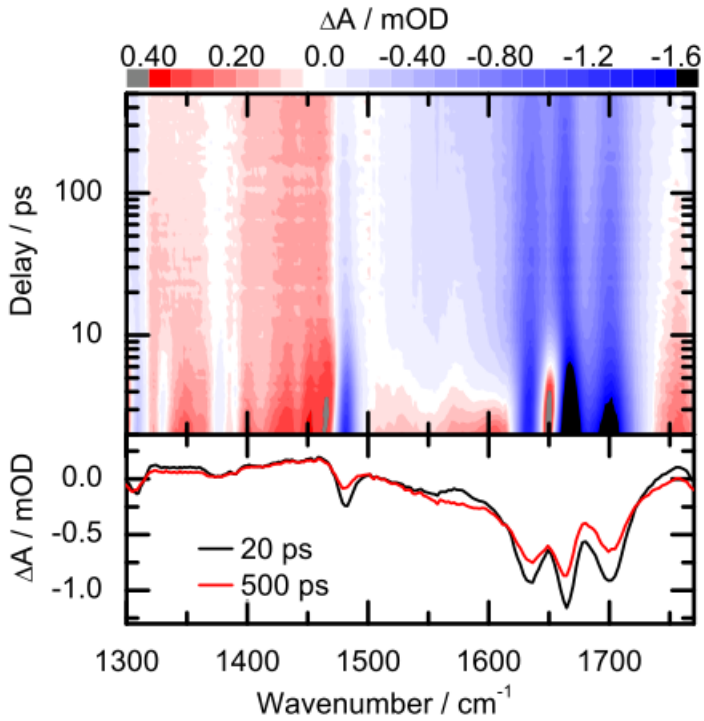

Figure S1. Transient absorption changes recorded for $(dT)_{18}$ after UV-excitation at 266 nm in D_2O buffered solution. Top: Contour plot representation of the experimental data. Positive absorption changes are indicated in red, negative absorption changes are indicated in blue. Bottom: Transient spectra at the indicated delay times.

A comparison of transient absorption changes recorded for $(dT)_{18}$ and TMP is given Figure S2. Panel (a) shows the transient spectra obtained 2 ns after excitation. In panel (b) the time traces at the maximum bleach signal at 1664 cm^{-1} are compared. Clearly, a strong 100 ps decay component is observed for $(dT)_{18}$ but such a component is absent for TMP.

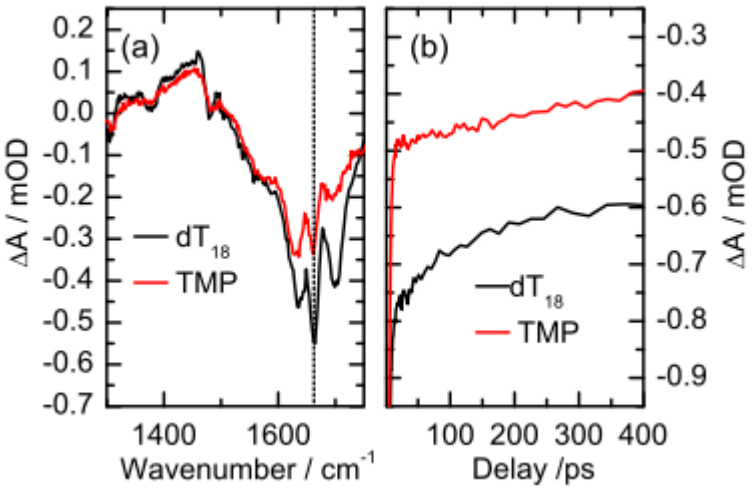

Figure S2. Transient absorption changes recorded for $(dT)_{18}$ and TMP after UV-excitation at 266 nm in D_2O buffered solution. (a) Transient spectra recorded 2 ns after excitation. (b) Time dependence of the absorption signal at the maximum bleach observed at 1664 cm^{-1} (indicated as dotted line in panel (a)).

3. Identification of CT Signature ($T^{\bullet+}\_T^{\bullet-}$)

For the assignment of the DAS(100 ps) signal obtained for $(dT)_{18}$ to a charge separated state we determined the expected signature (consisting of a thymine anion and cation) according to the following equation:

$$DAS(T^{\bullet+}\_T^{\bullet-}) = DAS(T^{\bullet-}A^{\bullet+}) - DAS(A^{\bullet+}) + DAS(T^{\bullet+}). \quad (1)$$

Application of this equation requires proper treatment of the experimental spectra. Obviously, the magnitude of the recorded decay associated spectra (DAS) depend on the excitation intensity. This must be accounted for. Further, the IR signature of a base is affected by its surrounding (stacked or not stacked). This also must be taken into consideration. Therefore, the procedure described in the following is more involved than the equation suggests.

The DAS for the decay of $T^{\bullet-}pA^{\bullet+}$ was obtained in a TRIR experiment on the dinucleotide TpA (see Figure S6a) were a charge transfer state with a lifetime of about 50 ps was observed. The assignment is based on a recent study by Doorley at al. [5] where a charge transfer state consisting of an adenine cation and a thymine anion ($A^{\bullet+}pT^{\bullet-}$) with a lifetime of 75 ps has been identified for the dinucleotide ApT. In our study, we verified the results from Doorley et al. on ApT and then performed experiments on TpA. In ApT and TpA similar charge transfer signatures were found indicating that in both dinucleotides an electron transfer from adenine to thymine occurs.

The signatures of the cations $T^{\bullet+}$ and $A^{\bullet+}$ were obtained in two-photon ionization experiments on $(dT)_{18}$ and $(dA)_{18}$, respectively. The oligomers $(dA)_{18}$ and $(dT)_{18}$ were used for this analysis, because their spectra are modified by stacking interactions, and charge transfer is expected for stacked bases. In these experiments long (1 ns) and short excitation pulses (200 fs) were applied. The high excitation intensity of the fs-excitation pulses results in a small amount of two-photon ionization that is not present with the comparably long ns pulse excitation. Subtraction of the ns from the fs data obtained for $(dT)_{18}$ yields the two-photon ionization signal shown in Figure S3.

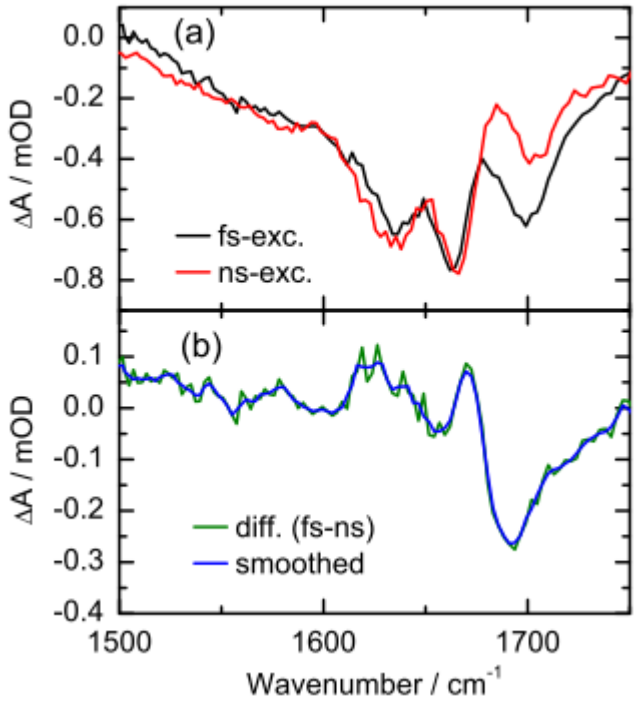

Figure S3: (a) Comparison of absorption changes recorded 2 ns after UV excitation of $(dT)_{18}$ with fs-pulses (black) and ns-pulses (red). (b) The calculated absorption difference between the two data sets (green) can be assigned to two-photon-ionization of thymine bases in $(dT)_{18}$. For further calculations the smoothed dataset (blue) was used.

In the case of $(dA)_{18}$ one-photon excitation signals decay on the 100 ps time scale, whereas longer lived signals on the ns time scale can be ascribed to two-photon ionization. Therefore, experiments with high intensity fs-excitation (about 4.5 µJ excitation energy, more than twice the intensity as in the actual experiment on $(dT)_{18}$) were performed and the residual absorption changes after 1 ns were recorded. The thus obtained signature is given as broken red line in Figure S5b.

Scaling of the spectra of the two cations and of $T^{\bullet-}pA^{\bullet+}$ relies on ground state bleaches. These bleaches are compared with (inverted) ground state IR spectra for which absorption coefficients are available. By overlapping the bleaches with the inverted IR spectra absorption coefficients for the positive transient absorption bands are obtained. Effects of the stacking on the IR spectra complicate this procedure.

To identifiy the effects of stacking interactions the IR absorption coefficients of adenine (left) and thymine (right) compounds are shown in Figure S4. Comparing AMP (blue) and $(dA)_{18}$ (red) a strong hypochromic effect of about 30 % and a significant spectral shift of the main

absorption band (assigned to C=C and C=N double bonds, see ref. [6]) from 1624 cm^{-1} for AMP to 1628 cm^{-1} for $(dA)_{18}$ is observed. The smaller absorption band around 1575 cm^{-1} exhibits a similar decrease in absorption, yet its position remains essentially unchanged. The differences between the monomer AMP and the oligomer $(dA)_{18}$ can be assigned to a significant amount of base stacking of adenine bases in $(dA)_{18}$. The latter is in line with results by Dewey and Turner who determined a fraction of about 80 % stacked bases for poly(dA).[7]

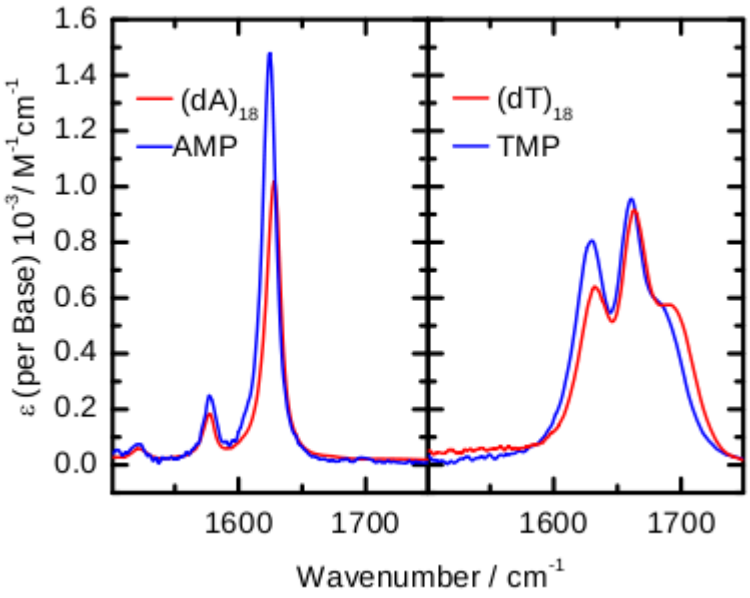

Figure S4: Comparison of absorption coefficients. Left: AMP and $(dA)_{18}$. Right: TMP and $(dT)_{18}$.

Comparing TMP (blue) and $(dT)_{18}$ (red) the absorption spectrum of $(dT)_{18}$ reveals a reduction around 1630 cm^{-1} (assigned to the C5=C6 double bond, see ref. [6]) and a small blue shift for the C4=O double bond above 1675 cm^{-1}. Yet, the absorption of the C2=O double bond located around 1664 cm^{-1} remains virtually unchanged under base interaction. The latter finding was used for the scaling of the TpA charge transfer signal and the cation obtained by two-photon ionization of $(dT)_{18}$. Thereby it was assumed that the base stacking interactions between thymine and adenine bases in TpA also do not alter the absorption coefficient of the C2=O double bond of the thymine base significantly. Under this premise the maximum bleach signal at 1664 cm^{-1} was used as marker for the scaling of the charge transfer signal of TpA ($DAS(T^{\bullet-}pA^{\bullet+})$) to the inverted ground state absorption coefficient of $(dT)_{18}$. The thymine cation signature ($T^{\bullet+}$) was scaled to fit the shoulder of the inverted ground state absorption coefficient of $(dT)_{18}$ above 1700 cm^{-1}.

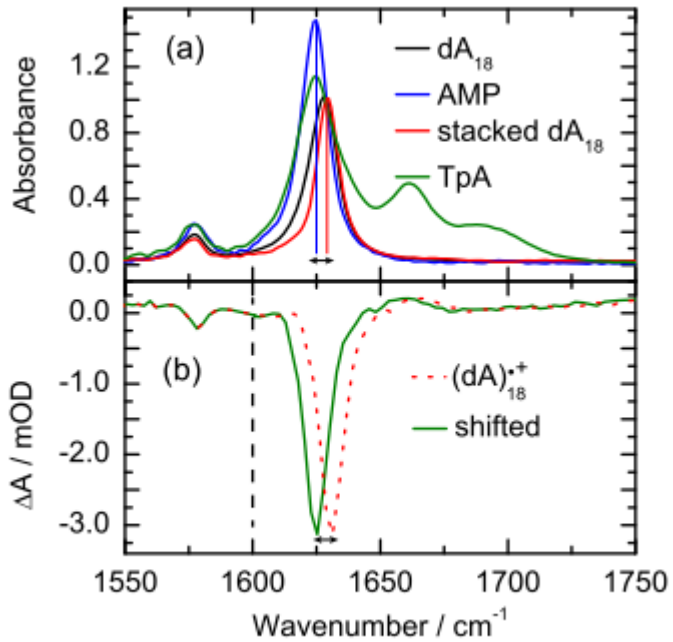

Figure S5: (a) Absorption coefficients for AMP and $(dA)_{18}$ (per base) and TpA (per dinucleotide). (b) Two-Photon ionization signature for $(dA)_{18}$ (dotted red line). To account for the different spectral shifts due to stacking interactions in $(dA)_{18}$ and TpA (see text) the spectral part above 1600cm^{-1} was red-shifted by 6 cm^{-1}, resulting in the green line. The latter is assigned as cation signature ($A^{\bullet+}$).

The appropriate scaling of the adenine cation signal obtained after two-photon ionization of $(dA)_{18}$ requires additional considerations. In Figure S5a the ground state IR spectra of AMP, $(dA)_{18}$ and TpA are compared. In $(dA)_{18}$ as well as in TpA, base stacking profoundly modifies the absorption coefficients. In $(dA)_{18}$ the peak position of the main adenine absorption (1628 cm^{-1}) is blue-shifted by 4 cm^{-1} in comparison to AMP and TpA, while the smaller absorption band around 1575 cm^{-1} does not show a significant shift at all.

In the study by Doorley et al. the IR absorption spectra for stacked and unstacked dinucleotide conformations of ApT were derived from ground state absorption spectra.[5] Comparison of the absorption spectra of the monomers AMP and TMP with ApT revealed a marked suppression of the adenine absorption and a red-shift of the absorption peak of AMP from 1624 cm^{-1} to about 1621 cm^{-1} for stacked adenine bases. Obviously spectral shifts due to stacking interactions in $(dA)_{18}$ strands (blue-shift) where two and more adenine bases can be stacked and in the dinucleotide TpA (red-shift) have to be taken into account differently.

Here, two assumptions have been made to obtain a reasonable adenine cation signal that can be applied to the dinucleotide TpA:

(i) To take into account the different spectral shifts for stacked bases in $(dA)_{18}$ and TpA the spectral part above 1600 cm^{-1} of the adenine cation signature has been red-shifted by 6 cm^{-1} (red line in Figure S5b). (ii) To account for the hypochromism observed for stacked adenine bases the absorption coefficient of the main IR absorption band of the adenine base was assumed to be of the same order as in $(dA)_{18}$ (about 1000 $M^{-1}cm^{-1}$ at 1628 cm-1). Scaling of the adenine cation signature was performed by matching the cation data and the inverted ground state absorption coefficient of $(dA)_{18}$.

By the scaling procedure values for the absorption coefficients of the cation and anion species were obtained and Lambert Beer's law was applied to calculate the respective absorbance changes. The scaled signatures are given in Figure S6. In panel (a) the DAS of ($T^{\bullet-}pA^{\bullet+}$) and the anion ($A^{\bullet+}$) are shown. Addition of ($T^{\bullet-}pA^{\bullet+}$) and ($A^{\bullet+}$) results in the anion signal ($T^{\bullet-}$) that is shown with the cation signal ($T^{\bullet+}$) in panel (b). In panel (c) the sum of the cation and anion thymine signals ($T^{\bullet+} + T^{\bullet-}$) is compared with the DAS(100 ps) signal obtained for $(dT)_{18}$.

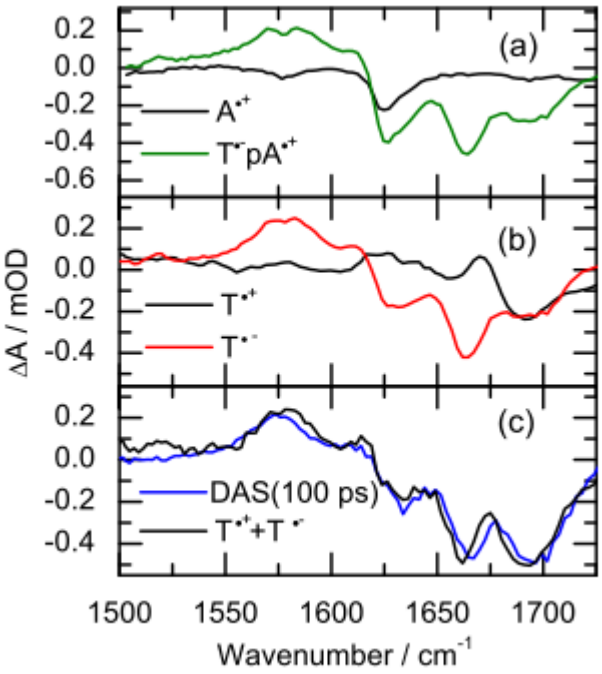

Figure S6: (a) DAS of ($T^{\bullet-}pA^{\bullet+}$) in green and the cation ($A^{\bullet+}$) in black. (b) Signatures of the cation ($T^{\bullet+}$) in black and the anion ($T^{\bullet-}$) in red. The latter was obtained as difference between ($T^{\bullet-}pA^{\bullet+}$) and ($A^{+}$). (c) Sum of the cation and anion thymine signatures ($T^{\bullet+} + T^{\bullet-}$) compared to DAS(100 ps) of $(dT)_{18}$

4. Quantum Yield of CT Formation

The quantum yield of charge transfer formation can be estimated by comparing the absorbance changes due to CT-state formation and the formation of CPD lesions. In Figure S7 the respective difference spectra are depicted together with the inverted ground state absorption spectrum of $(dT)_{18}$. For a direct comparison of the data that have been obtained in different measurements the transient data were first scaled to the amount of initially excited thymine bases by using the transient IR signal of the solvent D_2O (absorption changes induced by heating of the sample volume) as internal measure of the deposited energy [3]. Then the ground state spectrum was scaled to match the observed maximum bleach signatures at 1700 cm^{-1} (top, CT state) and 1630 cm^{-1} (bottom, CPD). In this way one can directly compare the amount of ground state bleach (GSB) associated with the different species. In the case of the CPD formation the applied scaling is supported by the fact that the absorption band peaking at 1630 cm^{-1} in $(dT)_{18}$ is attributed to the C5=C6 double bond that is missing in the CPD lesion. For the CT state the scaling to the maximum bleach at 1700 cm^{-1} represents a lower border assuming that the CT state does not show significant absorption above 1700 cm^{-1}. Yet, the later scaling also matches the GSB at 1480 cm^{-1} giving further support that the applied scaling represents a reasonable amount of GSB. Comparison of the in this way obtained ground state bleach spectra shows that the GSB due to the CT state is ca. 1.3 times higher than the GSB associated with CPD formation. Assuming a quantum yield Φ_{CPD} of 0.05 [8] this results in an estimated quantum yield Φ_{CT} of about 0.07.

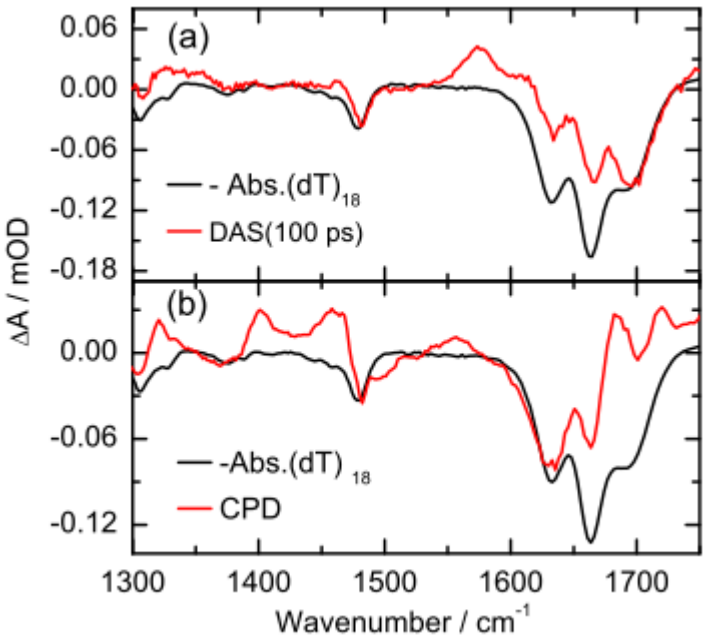

Figure S7: Comparison of absorption changes ΔA assigned to the decay of (a) CT-states DAS (100 ps) and (b) CPD formation. Inverted and scaled ground state spectra of $(dT)_{18}$ are given in black.

4. Estimates on Rate Constants for CT and Recombination

Experimental rate constants for charge transfer (CT) and recombination (RC) are here compared with predications from non-adiabatic electron transfer theory. A two-mode model is employed (see e.g. ref. [9]). In this model the rate constant for electron transfer k_{ET} is given by

$$k_{ET} = \frac{2\pi}{\hbar} V^2 \frac{1}{\sqrt{4\pi k_b T \lambda_s}} \sum_{m=0}^{\infty} \frac{S^m}{m!} e^{-S} e^{-\frac{(\Delta G + \lambda_s + m\hbar\omega)^2}{4 k_b T \lambda_s}}.$$

Hereby, V is the electronic coupling mediating the transfer, λ_s is the contribution of the solvent to the reorganization energy, $\hbar\omega$ is the energy of the effective vibrational mode associated with inner sphere reorganization. The energy of this reorganization λ_i enters the expression via the Huang-Rhys factor $S = \lambda_i / \hbar\omega$. The change in Gibbs free energy caused by the ET process is denoted by ΔG and $k_b T$ stands for the thermal energy.

The change ΔG can be obtained from spectroscopic and electrochemical data via the Weller equation (see e.g. ref.[10]). For the CT process starting from the excited singlet state the expression reads

$$\Delta G_{CT,s} = -E_{00,s} - e_0\left(E^{0}_{T,T^{\cdot-}} - E^{0}_{T^{\cdot+},T}\right) + \frac{e_0^2}{4\pi\varepsilon_o\varepsilon_r r}.$$

The first term $E_{00,s}$ is the energy of the singlet 0-0 transition of the thymine moiety. The second contains potentials for the one electron reduction and oxidation of the thymine moiety (e_0 is the elementary charge). In the last term – the work term – r is the distance of the two thymine moieties involved in the transfer, ε_0 is the vacuum permittivity, and ε_r is the dielectric constant. For the CT process starting from the excited triplet state the expression now includes $E_{00,t}$, the energy of the triplet 0-0 transition of the thymine moiety,

$$\Delta G_{CT,t} = -E_{00,t} - e_0\left(E^{0}_{T,T^{\cdot-}} - E^{0}_{T^{\cdot+},T}\right) + \frac{e_0^2}{4\pi\varepsilon_0\varepsilon_r r}.$$

The change in Gibbs free energy for the RC process is given by

$$\Delta G_{RC} = e_0\left(E^{0}_{T,T^{\cdot-}} - E^{0}_{T^{\cdot+},T}\right) - \frac{e_0^2}{4\pi\varepsilon_0\varepsilon_r r}.$$

The singlet energy $E_{00,S}$ may be obtained from absorption and fluorescence spectroscopy. Equating the average of the absorption and emission maximum of the respective spectra for

thymine in water (ref.[11]) with $E_{00,s}$ yields a value of 4.22 eV. The energy of the lowest triplet state of thymine $E_{00,t}$ as measured by phosphorescence spectroscopy at low temperature amounts to 3.27 eV (see compilation of data in ref.[12]).

Finding the correct values for the reduction potentials is more involved. Upon photoexcitation of $(dT)_{18}$ the following electron transfer processes between adjacent bases are assumed to occur

$$\cdots T^{*} - T \cdots \xrightarrow{k_{CT}} \cdots T^{\cdot +} - T^{\cdot -} \cdots \xrightarrow{k_{RC}} \cdots T - T \cdots,$$

i.e. only electrons are transferred and this transfer is not accompanied by the transfer of protons. We note that proton coupled electron transfer processes have been discussed in relation with charge transfer processes in DNA (see e.g. ref.[13]). Computing the free energy differences for such "electron only transfers" requires reduction potentials for these two processes:

$T + e^{-} \rightarrow T^{\cdot -}$ $\quad E^{0}_{T,T^{\cdot -}}$

$T^{\cdot +} + e^{-} \rightarrow T$ $\quad E^{0}_{T^{\cdot +},T}$

In the experiments reported here, $(dT)_{18}$ was dissolved in aqueous solution and thus potentials for these conditions are required. Electrochemical measurements on the DNA bases in water are hampered by the limited potential range and acid-base equilibria affecting these potentials (for pKa's of the bases and their radicals see ref.[14]). To avoid these complications, Seidel et al. determined these potentials in the aprotic solvents acetonitrile and dimethylformamide and "converted" the results to water using the Born equation.[15] Their values are -2.21 V (all potentials versus NHE) for $E^{0}_{T,T^{\cdot -}}$ and +2.08 V for $E^{0}_{T^{\cdot +},T}$. Steenken et al. conducted measurements in water and report a less negative value for $E^{0}_{T,T^{\cdot -}}$ (-1.1 V).[16] Based on the pertinent pK_a they argue that for the slightly alkalic conditions the employed protonation of the radical anion should not come into play. The difference might be due to hydrogen bonding not accounted for in the Born model. For $E^{0}_{T^{\cdot +},T}$ Steenken et al. (see ref.[17]) report a less positive value (+1.7 V) than Seidel et al.. Steenken et al. worked in aqueous solution at pH 7. Since oxidized thymine $T^{\cdot +}$ is a relatively strong acid (pK_a of 3.6, ref.[14]), acid-base equilibrium will affect the potential. In a recent quantum chemical study (ref.[18]) a potential for the oxidation coupled to the de-protonation and the pK_a values were computed. These values yield a potential $E^{0}_{T^{+},T}$ of +2.3 V. From this survey of the literature inserting -1.1 V for $E^{0}_{T,T^{\cdot -}}$ and +2.3 V for $E^{0}_{T^{\cdot +},T}$ into the expressions for the free energy differences seems appropriate.

Evaluation of the work term requires the distance r between two adjacent thymine moieties. According to molecular dynamics simulations on TpT in water (see ref.[19]) the probability density for this distance peaks at 4.3 Å. Based on this distance a work term of 0.04 eV is computed which – particularly in the light of the uncertainties of reduction potentials – may be neglected (see ref. [11]). The ΔG values and other parameters entering the computation of the rate constants are compiled in Table 1.

Process	ΔG [eV]	λ_s [eV]	λ_i [eV]	$\hbar\omega$ [cm^{-1}]	V [cm^{-1}]
CT, S	-0.81	1.12	0.88	1500	50
CT, T	+0.13	1.12	0.88	1500	50
RC	-3.40	1.12	0.88	1500	50

Table 1: Compilation of parameters entering the computation of the rate constants. For references see text.

Kao et al. recently studied the electron transfer in a related system.[11] In the system the electron is transferred between a photo-excited tryptophan moiety which is covalently linked to a thymine moiety. For this system and water as solvent they derive a total reorganization energy λ_t of ~ 2 eV. We separate the reorganization energy into the solvent part λ_s and the inner sphere part λ_i. The latter can be obtained from the differences between adiabatic and vertical ionization energies (λ_i^+) as well as electron affinities (λ_i^-) (see ref. [20]). The contribution λ_i^+ amounts to 0.27 eV (ref. [20]), the λ_i^- part to 0.61 eV (ref. [21]) and the sum λ_i to 0.88 eV. This leaves 1.12 eV for the solvent part λ_s. (Marcus' expression for this quantity (see eq. (11) in ref. [11]) predicts a larger value of ~ 2 eV). However, the expression tends to overestimate the solvent reorganization here (see discussion in ref. [11])). In a recent time dependent DFT computation on TpT in water (treated as a polarizable continuum) the adiabatic energy of the CT state was located at 3.4 eV.[8] Neglecting entropy differences, this adiabatic energy should equal $|\Delta G_{RC}|$ which (see Table 1) is indeed the case. The vertical excitation energy should approximately be given by $|\Delta G_{RC}| + \lambda_t$ (see chapter 9 in ref. [22]). The time dependent DFT computations result in a value of 5.5 eV for the vertical excitation and thus 2.1 eV for λ_t. The time dependent DFT computation (ref. [8]) is by several tenths of an electron volt off the experimental value for the singlet excitation of thymine. Therefore, the nearly exact agreement between the values derived from spectroscopy or electrochemistry and the computed ones should not be given too much significance.

Concerning the energy of the vibrational quantum $\hbar\omega$ we follow the common convention and set it to 1500 cm^{-1} (ref.[23]). Assuming that the reorganization energies and the electronic coupling V apply for all three processes their rate constants for room temperature may now be computed provided that V is available. For related systems (refs.[11, 23]) couplings of around 50 cm^{-1} were obtained. Inserting these values yields the following rate constants:

$k_{CT,s} = 6.7 \cdot 10^9\ s^{-1}$ (experiment $10^{11}\ s^{-1}$);

$k_{CT,t} = 5.2 \cdot 10^3\ s^{-1}$ (experiment $< 10^8\ s^{-1}$, ref.[24]);

$k_{RC} = 6.8 \cdot 10^9\ s^{-1}$ (experiment $10^{10}\ s^{-1}$).

This estimate supports the notion that ET originating from the triplet state cannot be observed since its rate constant is computed to be orders of magnitude smaller than the one for the biradical formation. The computed rate constants $k_{CT,s}$ and k_{RC} are by factors of around 15 and 1.5 short of the experimental values. In the light of the uncertainties for parameters entering the computation this is not surprising. By allowing for variations of these parameters the experimental values may be approached. Furthermore, it may not be excluded that different values for the electronic coupling and the reorganization energies ought to be inserted for the three ET process (see e.g. discussion in ref.[25]). This would further increase the number of adjustable parameters. Since only two experimental rate constants are available to derive the other parameters we refrain from such variation. Nonetheless, this analysis indicates that the spectral signatures (Figure 1 in the main text) as well as the rate constants are in line with an ET process occurring in photo-excited $(dT)_{18}$.

References

1. T. Schrader, A. Sieg, F. Koller, W. Schreier, Q. An, W. Zinth and P. Gilch, *Chem. Phys. Lett.*, 2004, **392**, 358-364.
2. G. Ryseck, T. Schmierer, K. Haiser, W. J. Schreier, W. Zinth and P. Gilch, *ChemPhysChem*, 2011, **12**, 1880-1888.
3. K. Haiser, B. P. Fingerhut, K. Heil, A. Glas, T. T. Herzog, B. M. Pilles, W. J. Schreier, W. Zinth, R. de Vivie-Riedle and T. Carell, *Angew. Chem. Int. Ed.*, 2012, **51**, 408-411.
4. M. Towrie, G. W. Doorley, M. W. George, A. W. Parker, S. J. Quinn and J. M. Kelly, *Analyst*, 2009, **134**, 1265-1273.
5. G. W. Doorley, M. Wojdyla, G. W. Watson, M. Towrie, A. W. Parker, J. M. Kelly and S. J. Quinn, *J. Phys. Chem. Lett.*, 2013, **4**, 2739-2744.
6. M. Banyay, M. Sarkar and A. Graslund, *Biophys. Chem.*, 2003, **104**, 477-488.
7. T. G. Dewey and D. H. Turner, *Biochemistry*, 1979, **18**, 5757-5762.
8. A. Banyasz, T. Douki, R. Improta, T. Gustavsson, D. Onidas, I. Vaya, M. Perron and D. Markovitsi, *J. Am. Chem. Soc.*, 2012, **134**, 14834-14845.
9. M. Bixon and J. Jortner, *The Journal of Physical Chemistry*, 1991, **95**, 1941-1944.

10. G. J. Kavarnos and N. J. Turro, *Chem.Rev.*, 1986, **86**, 401-449.
11. Y.-T. Kao, X. Guo, Y. Yang, Z. Liu, A. Hassanali, Q.-H. Song, L. Wang and D. Zhong, *J. Phys. Chem. B*, 2012, **116**, 9130-9140.
12. M. C. Cuquerella, V. Lhiaubet-Vallet, F. Bosca and M. A. Miranda, *Chem. Sci.*, 2011, **2**, 1219-1232.
13. S. Steenken, *Biol. Chem.*, 1997, **378**, 1293-1297.
14. D. M. Close, W. H. Nelson and W. A. Bernhard, *J. Phys. Chem. A*, 2013, **117**, 12608-12615.
15. C. A. M. Seidel, A. Schulz and M. H. M. Sauer, *J. Phys. Chem.*, 1996, **100**, 5541-5553.
16. S. Steenken, J. P. Telo, H. M. Novais and L. P. Candeias, *J. Am. Chem. Soc.*, 1992, **114**, 4701-4709.
17. S. Steenken and S. V. Jovanovic, *J. Am. Chem. Soc.*, 1997, **119**, 617-618.
18. B. T. Psciuk, R. L. Lord, B. H. Munk and H. B. Schlegel, *J. Chem. Theory Comput.*, 2012, **8**, 5107-5123.
19. Y. K. Law, J. Azadi, C. E. Crespo-Hernandez, E. Olmon and B. Kohler, *Biophys. J.*, 2008, **94**, 3590-3600.
20. J. Olofsson and S. Larsson, *J. Phys. Chem. B*, 2001, **105**, 10398-10406.
21. S. Kim, S. E. Wheeler and H. F. Schaefer, *The Journal of Chemical Physics*, 2006, **124**, 204310.
22. A. M. Kuznetsov and J. Ulstrup, *Electron Transfer in Chemistry and Biology: An Introduction to the Theory*, Wiley & Sons, 1999.
23. D. N. LeBard, M. Lilichenko, D. V. Matyushov, Y. A. Berlin and M. A. Ratner, *The Journal of Physical Chemistry B*, 2003, **107**, 14509-14520.
24. B. M. Pilles, D. B. Bucher, L. Liu, P. Clivio, P. Gilch, W. Zinth and W. J. Schreier, *J. Phys. Chem. Lett.*, 2014, **5**, 1616-1622.
25. F. D. Lewis, R. S. Kalgutkar, Y. Wu, X. Liu, J. Liu, R. T. Hayes, S. E. Miller and M. R. Wasielewski, *J. Am. Chem. Soc.*, 2000, **122**, 12346-12351.